Mechanism and Utility of an RNA-Cleaving DNA Enzyme[†]

Stephen W. Santoro and Gerald F. Joyce*

Departments of Chemistry and Molecular Biology and The Skaggs Institute for Chemical Biology, The Scripps Research Institute, 10550 North Torrey Pines Road, La Jolla, California 92037

Received May 22, 1998; Revised Manuscript Received July 23, 1998

ABSTRACT: We previously reported the in vitro selection of a general-purpose RNA-cleaving DNA enzyme that exhibits a catalytic efficiency (k_{cat}/K_M) exceeding that of any other known nucleic acid enzyme [Santoro, S. W. and Joyce, G. F. (1997) *Proc. Natl. Acad. Sci. U.S.A. 94*, 4262−4266]. This enzyme contains ∼30 deoxynucleotides and can cleave almost any RNA substrate under simulated physiological conditions, recognizing the substrate through two Watson−Crick binding domains. The kinetics of cleavage under conditions of varying pH, choice of divalent metal cofactor, and divalent metal concentration are consistent with a chemical mechanism involving metal-assisted deprotonation of a 2′-hydroxyl of the substrate, leading to substrate cleavage. Kinetic measurements reveal that the enzyme strongly prefers cleavage of the substrate over ligation of the two cleavage products and that the enzyme's catalytic efficiency is limited by the rate of substrate binding. The enzyme displays a high level of substrate specificity, discriminating against RNAs that contain a single base mismatch within either of the two substrate-recognition domains. With appropriate design of the substrate-recognition domains, the enzyme exhibits a potent combination of high substrate sequence specificity and selectivity, high catalytic efficiency, and rapid catalytic turnover.

Nucleic acid enzymes have proven themselves particularly adept at catalyzing the sequence-specific cleavage of RNA. A variety of ribozymes that perform this function have been discovered in nature and studied extensively in the laboratory, including the hammerhead, hairpin, and group I catalytic motifs (for reviews, see *1*−*3*). Several years ago it was shown that certain DNA molecules, selected from a large random pool, also can catalyze the cleavage of an RNA phosphoester (*4*). More recently, the selection and initial characterization of a highly efficient, general-purpose RNA-cleaving DNA enzyme were reported (*5*). This molecule was identified from a population of $\sim 10^{14}$ different DNA molecules following 10 successive rounds of in vitro selective amplification. The selection procedure was designed to enrich the population with individuals that best promoted the Mg^{2+}-dependent cleavage of 1 of 12 target ribonucleotides located within a substrate domain that was attached to the potential catalytic domain. Following the selection process, the catalytic and substrate domains were separated, allowing the DNA to function as a true enzyme, capable of sequence-specific, multiple-turnover cleavage of RNA.

The selected molecule is referred to as the "10-23 DNA enzyme", derived from the 23rd clone obtained after the 10th round of selective amplification (*5*). It is composed of a catalytic domain of 15 deoxynucleotides, flanked by 2 substrate-recognition domains of ∼8 nucleotides each. The recognition domains provide both the sequence information necessary to specify a particular RNA substrate and the binding energy to hold that substrate within the active site of the enzyme. As diagrammed in Figure 1, the enzyme (E) binds the substrate (S) through Watson−Crick base pairing and cleaves a particular phosphodiester linkage located between an unpaired purine and paired pyrimidine residue. This results in the formation of 5′ and 3′ products (P1 and P2), which contain a 2′,3′-cyclic phosphate and 5′-hydroxyl terminus, respectively. By appropriately designing the sequences of the two substrate-recognition domains, the enzyme can be made to cleave virtually any RNA that contains a purine−pyrimidine junction.

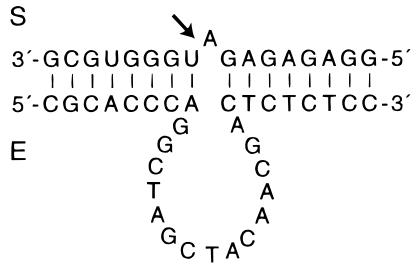

FIGURE 1: RNA cleavage catalyzed by the 10-23 DNA enzyme. The DNA enzyme (E) binds an RNA substrate (S) through two substrate-recognition domains, each involving Watson−Crick base pairing. The substrate corresponds in sequence to the region surrounding the start codon of HIV-1 *gag-pol* mRNA. The arrow indicates the site of substrate cleavage. Cleavage results in the formation of a 5′ and 3′ product (P1 and P2, respectively).

Under multiple-turnover conditions, the 10-23 DNA enzyme exhibits Michaelis−Menten kinetics, with a k_{cat} of ~ 0.1 min^{-1} and K_M of ∼1 nM when measured in the presence of 2 mM $MgCl_2$ and 150 mM NaCl at pH 7.5 and 37 °C (*5*). Under conditions of higher pH and/or modified divalent cation conditions, the enzyme can cleave with a k_{cat} of ~ 10 min^{-1} and a catalytic efficiency, k_{cat}/K_M, of $> 10^9$ M^{-1} min^{-1}.

[†] Supported by Research Grant SFP-1076 from Johnson & Johnson Research and Research Grant AI30882 from the National Institutes of Health.

* To whom correspondence should be addressed.

S0006-2960(98)01222-7 CCC: $15.00
Published on Web 08/29/1998

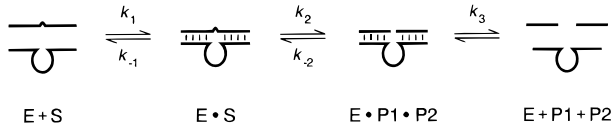

FIGURE 2: Minimal kinetic scheme for catalysis by the 10-23 DNA enzyme. For simplicity, k_3 represents the rate constant for release of the product that dissociates most slowly from the enzyme.

The characteristics of the 10-23 DNA enzyme make it an attractive tool for use as a sequence-specific endoribonuclease, both in vitro and in vivo. The goal of the present study was to characterize more fully the catalytic properties of this enzyme in order to facilitate its application to a broad range of RNA targets. Kinetic analysis of the enzyme in the presence of saturating concentrations of substrate demonstrated that the catalytic rate increases log-linearly with increasing pH, consistent with a chemical mechanism involving rate-limiting deprotonation of the 2′-hydroxyl adjacent to the cleavage site. The catalytic rate also increases approximately linearly with increasing concentration of various divalent metal cations, consistent with a chemical mechanism involving metal-assisted deprotonation of the 2′-hydroxyl adjacent to the cleavage site.

The minimal kinetic scheme for one turnover of the enzyme (Figure 2) involves binding of E and S to form a productive enzyme−substrate complex (E·S), cleavage of S to form an enzyme−product complex (E·P1·P2), and release of the products to regenerate the free enzyme. These steps proceed with rate constants k_1, k_2, and k_3, respectively, each step being reversible. Kinetic analysis of the reverse reaction (product ligation) revealed that the enzyme has a strong preference for substrate cleavage over product ligation. Examination of the rate of enzyme−substrate association (k_1) provided an understanding of the basis for the enzyme's high catalytic efficiency in comparison to analogous RNA enzymes such as the hammerhead and group I ribozymes. The catalytic efficiency of the DNA enzyme is determined by the rate of enzyme−substrate association, which in turn is limited by the rate of helical nucleation of the corresponding DNA−RNA heteroduplex. It appears that, unlike the hammerhead and group I ribozymes, the 10-23 DNA enzyme takes full advantage of the inherent rate of duplex formation, presumably by avoiding alternative structures that would limit the rate of substrate binding.

The ability of the DNA enzyme to cleave a particular target RNA was examined with respect to the sequence at the cleavage site, the length of the substrate-recognition domains, and the substrate sequence specificity of the reaction. Kinetic parameters for the cleavage of RNA substrates that differed only at the nucleotide position located immediately to the 5′ side of the cleavage site demonstrated that substrates containing an unpaired purine at that position are cleaved most rapidly. An investigation of the catalytic activity of the DNA enzyme as a function of the lengths of its substrate-recognition domains, and consideration of calculated values for the binding energy of substrate and product with these various enzymes, suggested a simple framework for the design of recognition domains that provide optimal catalytic efficiency, catalytic turnover rate, substrate sequence specificity, and substrate sequence selectivity. Substrate sequence specificity was examined for a DNA enzyme with substrate-recognition domains of optimal length. In general, single mismatches resulted in substantial reduction of the enzyme's catalytic efficiency, demonstrating the high degree of sequence specificity that is provided by the two substrate-recognition domains.

The DNA enzyme is a biologically familiar macromolecule with polyanionic character. As a result, its application to biological systems faces special obstacles with regard to compound delivery and stability. On the other hand, the synthesis of a DNA enzyme is easily within reach of most laboratories. The target sequence generality and favorable catalytic properties of the 10-23 DNA enzyme distinguish it as a potentially useful reagent for the manipulation of RNA.

MATERIALS AND METHODS

Preparation of Oligonucleotides. Unless stated otherwise, all experiments employed a 31-nucleotide DNA enzyme (E) with substrate-recognition domains of 8 nucleotides each (8+8) and a 17-nucleotide RNA substrate (S) corresponding to the region surrounding the start codon of HIV-1 *gag-pol* mRNA (Figure 1). Synthetic RNA substrates, RNA antisense oligonucleotides, and 3′ RNA product (P2) were synthesized using a Pharmacia Gene Assembler Special automated DNA/RNA synthesizer and deprotected as described previously (*6*). In vitro transcribed substrates were prepared using T7 RNA polymerase and synthetic DNA templates (*7*). DNA enzymes, complementary DNA oligonucleotides, and DNA templates for transcription were prepared by Operon Technologies (Alameda, CA).

RNA and DNA oligonucleotides were purified by denaturing polyacrylamide gel electrophoresis, followed by electroelution and ethanol precipitation. In vitro transcribed RNA substrates were dephosphorylated in a 250-μL reaction mixture containing 1 nmol of RNA, 50 mM tris(hydroxymethyl)aminomethane (Tris; pH 8.0), 0.4 mM disodium ethylenediaminetetraacetate (Na_2EDTA), and 0.2 unit/μL alkaline phosphatase, which was incubated at 37 °C for 1 h, extracted with phenol and chloroform, and ethanol precipitated. RNA substrates were 5′-^{32}P-labeled in a 10-μL reaction mixture containing 10 pmol of RNA, 40 pmol of [γ-^{32}P]ATP (7 μCi/pmol), 5 mM $MgCl_2$, 25 mM 2-(*N*-cyclohexylamino)ethanesulfonic acid (CHES; pH 9.0), 3 mM dithiothreitol (DTT), and 1.25 units/μL T4 polynucleotide kinase, which was incubated at 37 °C for 1 h. The labeled substrates were purified by denaturing polyacrylamide gel electrophoresis, followed by electroelution and ethanol precipitation. The 5′-^{32}P-labeled 5′ RNA product (P1) was obtained by incubating 2.5 pmol of 5′-^{32}P-labeled substrate in a 50-μL reaction mixture containing 100 nM E, 10 mM $CaCl_2$, 150 mM NaCl, 50 mM *N*-(2-hydroxyethyl)piperazine-*N*′-3-propanesulfonic acid (EPPS; pH 7.5), and 40 μg/mL bovine serum albumin (BSA) at 37 °C for 15 min, and was purified by denaturing polyacrylamide gel electrophoresis, followed by electroelution and ethanol precipitation. BSA, rather than sodium dodecyl sulfate (SDS), was employed in the presence of Ca^{2+} to avoid formation of insoluble SDS−Ca^{2+} complexes. Concentrations of unlabeled oligonucleotides were determined spectrophotometrically, and those of 5′-^{32}P-labeled substrates were determined by scintillation counting.

Determination of Reaction Rates and Equilibrium Constants. Unless otherwise indicated, all reactions were carried

out in the presence of 2 mM $MgCl_2$, 150 mM NaCl, 50 mM EPPS (pH 7.5), and 0.01% SDS at 37 °C. The pH of the stock solution of buffer was adjusted in reference to the final reaction mixture at 37 °C. Reactions were initiated by combining separate solutions of E and S, each containing the final concentration of buffer and salts at 37 °C. Aliquots were removed from the reaction mixture at various times and quenched by their addition to an equal to or greater volume of an ice-cold mixture containing 8 M urea, 20% sucrose, 90 mM Tris−borate (pH 8.3), Na_2EDTA in 2-fold excess over divalent metal ion concentration, 0.05% xylene cyanol, 0.05% bromophenol blue, and 0.1% SDS. Radiolabeled substrates and products were separated by denaturing polyacrylamide gel electrophoresis and quantitated using a Molecular Dynamics Phosphorimager.

For reactions carried out under multiple-turnover (excess substrate) conditions, a k_{obs} value was obtained for each [S] from a best-fit line, typically based on five data points obtained over the first 10% of the reaction. k_{cat} and K_M values were determined from the *y*-intercept and negative slope, respectively, of the best-fit line to a modified Eadie−Hofstee plot of k_{obs} versus k_{obs}/[S]. Each plot consisted of 10 data points for values of [S] that typically ranged from ≥10-fold below to ≥10-fold above K_M, with [S] always in ≥10-fold excess over [E].

Observed rate constants for single-turnover reactions were obtained from a curve fitted to a plot of fraction reacted versus time, based on the equation $y = x(1 - e^{-kt})$, where *y* is the fraction reacted at time *t*, *x* is the fraction reacted at $t = \infty$, and *k* is the observed rate constant. Kinetic values typically exhibited <20% variation for identical experiments performed on different days.

Analysis of Divalent Metal Cation Dependence. The rate of substrate cleavage, k_2, for the 10-23 DNA enzyme in the presence of either Pb^{2+}, Zn^{2+}, Cd^{2+}, Mn^{2+}, Mg^{2+}, Ca^{2+}, Sr^{2+}, Ba^{2+}, or Co^{2+} was measured under single-turnover conditions. Reactions were carried out in the presence of a 50 mM concentration of either Tris or EPPS buffer, with 1 μM E, 10 nM [5′-^{32}P]S, 10 mM M^{2+} (or 1 mM for Pb^{2+}), and 150 mM NaCl, at pH 7.5 and 37 °C. The dependence of k_2 on the concentration of divalent metal cation was determined for reactions conducted in the presence of either Ca^{2+} or Mn^{2+} under multiple-turnover conditions. k_{obs} for cleavage was measured in the presence of 100 nM S, 0.1−10 nM E, either 2−300 mM $CaCl_2$ or 0.01−20 mM $MnCl_2$, and 50 mM EPPS (pH 7.5) at 37 °C. Under these conditions, S is saturating and k_2 is rate-limiting for the catalytic cycle. The concentration of either Ca^{2+} or Mn^{2+} required for half-maximal activity was determined from a curve fitted to a plot of k_{obs} versus $[M^{2+}]$, based on the equation $k_{obs} = [M^{2+}]k_{max}/([M^{2+}] + K_d)$, where k_{max} is k_2 in the presence of saturating concentrations of divalent metal cation and K_d is the apparent dissociation constant for the divalent metal cation.

Analysis of pH Dependence. The dependence of k_2 on pH was analyzed under multiple-turnover conditions in the presence of 100 nM S, 0.2−10 nM E, 10 mM $CaCl_2$, and 50 mM buffer (pH 6.1−9.7) at 37 °C. The pH range for reactions buffered by 1,4-piperazinediethanesulfonic acid (PIPES) was 6.1−7.5, by EPPS was 7.1−8.5, and by 1,3-bis[tris(hydroxymethyl)methylamino]propane (bis-Tris propane) was 6.4−9.7. Under the chosen reaction conditions, [S] was saturating so that $k_{obs} = k_2$.

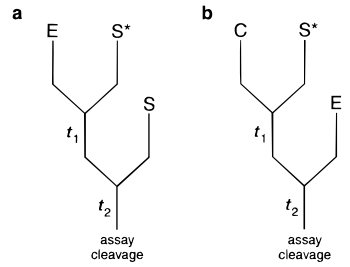

FIGURE 3: Scheme for pulse−chase experiments used to determine association rates involving RNA substrates. (a) Scheme for determination of enzyme−substrate association rates. S* corresponds to 5′-^{32}P-labeled substrate. (b) Scheme for determination of duplex formation rates. C corresponds to a complementary DNA oligonucleotide.

Determination of Reverse Reaction Rate. The reverse reaction was carried out by formation of the enzyme−product complex (E·P1·P2) in an 18-μL mixture containing 1.33 μM E, 4 nM 5′-^{32}P-labeled P1, and 2.67 μM P2, which was heated to 95 °C for 2 min and allowed to cool to 37 °C over 5 min, followed by addition of 6 μL of a solution containing 8 mM $MgCl_2$, 600 mM NaCl, 200 mM EPPS (pH 7.5), and 0.04% SDS. Two-microliter samples were removed and quenched at times ranging from 15 s to 60 min. The reaction also was carried out using 4-fold higher concentrations of E and P2 to ensure that E was saturated with respect to P2 and that P1 was saturated with respect to E·P2. The observed rate constant for the approach to equilibrium was determined as described above for single-turnover reactions. The values for K_{eq}^{int} and k_{-2} were determined from the final extent of the ligation reaction and the observed rate constant, as described under Results.

Estimation of Enzyme−Substrate Dissociation Rate. The upper limit for the rate of enzyme−substrate dissociation, k_{-1}, was determined by pulse−chase experiments (*8*−*10*). Seven microliter of a 200 nM solution of E in reaction buffer was combined with 7 μL of a 10 nM solution of [5′-^{32}P]S, also in reaction buffer. After an initial binding period, t_1, of 30 s, 14 μL of a 2 μM solution of unlabeled S in reaction buffer was added to initiate the chase. The period t_1 allowed nearly complete binding of [5′-^{32}P]S by E because it was >10-fold longer than the half-time for formation of E·S under these reaction conditions. Three-microliter aliquots were removed and quenched during the chase period, t_2, at times ranging from 90 s to 90 min. A control reaction in which no chase was added was carried out in parallel. The extent of cleavage for each reaction was determined as described above for single-turnover reactions.

Determination of Enzyme−Substrate Association Rate. The rate constant for enzyme−substrate association, k_1, was determined by pulse−chase experiments, carried out in the presence of either 2 or 100 mM Mg^{2+} (Figure 3a). Enzyme−substrate association was measured by observing substrate cleavage by the enzyme (*8*−*10*). For experiments with 2 mM Mg^{2+}, 10 different reactions were initiated by combining 17.5 μL of E in reaction buffer with 17.5 μL of [5′-^{32}P]S, also in reaction buffer, giving final concentrations of E of 0.5−5 nM and [5′-^{32}P]S of 0.1 nM. For experiments conducted with 100 mM Mg^{2+}, the final concentration of E was 0.05−0.5 nM, and [5′-^{32}P]S concentration was 0.01 nM.

Chases were initiated at various times, t_1, ranging from 10 s to 10 min, by combining 4-μL samples of each reaction mixture with 2 μL of 10 μM unlabeled S. The reactions were quenched after an interval, t_2, of 60 min. For each reaction, an observed rate constant was determined as described above for single-turnover reactions. The values for k_1 were determined from the observed rate constants, as described under Results.

Determination of Duplex Formation Rate. Rate constants for the association of complementary DNA or RNA oligonucleotides with various RNA substrates were determined by pulse−chase experiments, carried out in the presence of either 2 or 100 mM Mg^{2+}(Figure 3b). Duplex formation was measured by observing protection of the substrate from cleavage by the DNA enzyme. In addition to the standard substrate, measurements were obtained for three other RNA substrates having the sequences 5′-CAGUGGCAAUGAGAGUG-3′, 5′-GAGGAUAGAUGGAACAA-3′, and 5′-AGCCGAUGUGUGAGAAGAC-3′. For experiments with 2 mM Mg^{2+}, five different reactions were initiated by combining 17.5 μL of complementary oligonucleotide in reaction buffer with 17.5 μL of [5′-^{32}P]S, also in reaction buffer, giving a final concentration of complementary oligonucleotide of 0.5−5 nM and [5′-^{32}P]S of 0.1 nM. For experiments conducted with 100 mM Mg^{2+}, the final concentrations were 0.05−0.5 nM and 0.01 nM, respectively. Chases were initiated at various times, t_1, ranging from 10 s to 10 min, by combining 4-μL samples of each reaction mixture with 2 μL of 10 μM E in buffer containing 300 mM $MgCl_2$, 150 mM NaCl, and 50 mM EPPS (pH 7.5) at 37 °C. The reactions were quenched after an interval, t_2, of 30 min with 12 μL of a solution containing 100 mM Na_2EDTA. The observed rate constants were obtained from a curve fitted to a plot of fraction uncleaved versus time, based on the equation $y = x(1 - e^{-kt}) + m$, where y is the fraction reacted at time t, x is the fraction reacted at $t = \infty$, k is the observed rate constant, and m is the maximal extent of cleavage. The values for k_{assoc} were determined from the observed rate constants, as described under Results.

Analysis of the Effect of Varying Substrate-Recognition Domain Length. DNA enzymes were prepared with substrate-recognition domains of symmetrical length ranging from 4+4 to 13+13. For each enzyme, k_{obs} values were obtained from a best-fit line applied to data acquired during the steady-state portion of the reaction for cleavage of a 27mer synthetic RNA substrate having the sequence 5′-UAGAAGGAGAGAGAUGGGUGCGAGAGC-3′. k_{cat} and K_M values were determined as described above for multiple-turnover reactions.

RESULTS

Steady-State Catalytic Parameters. The rate of catalytic turnover, k_{cat}, and the Michaelis constant, K_M, for RNA cleavage by the 10-23 DNA enzyme were determined under multiple-turnover conditions in the presence of either 2 or 100 mM Mg^{2+} at pH 7.5 and 37 °C. Values for k_{cat} were 0.18 and 1.7 min^{-1} in the presence of 2 and 100 mM Mg^{2+}, respectively. These values are identical to the rate of substrate cleavage, k_2, measured under single-turnover conditions, demonstrating that product release, k_3, is not the rate-limiting step of the catalytic cycle under these conditions. Values for K_M were 0.62 and 0.35 nM in the presence of 2 and 100 mM Mg^{2+}, respectively. The catalytic efficiency, k_{cat}/K_M, of the DNA enzyme is 3.2×10^8 and 4.9×10^9 M^{-1} min^{-1} in the presence of 2 and 100 mM Mg^{2+}, respectively.

Dependence of Activity on Divalent Metal Ions and pH. The rate of DNA-catalyzed RNA cleavage, k_2, was assayed under single-turnover conditions in the presence of nine different divalent metal cations: Pb^{2+}, Zn^{2+}, Cd^{2+}, Mn^{2+}, Mg^{2+}, Ca^{2+}, Sr^{2+}, Ba^{2+}, and Co^{2+}. In each case, activity was measured in the presence of two different buffers, Tris and EPPS, at pH 7.5 and 37 °C. Two of the metals exhibited substantially different behavior in the presence of the two different buffers. Mn^{2+} provided the highest level of activity of all metals tested in the presence of EPPS, but very little activity in the presence of Tris. Cd^{2+} provided a modest level of activity in Tris, but very little activity in EPPS. The causes of these differences are unknown. These exceptions notwithstanding, the order of activity was as follows: Mn^{2+} (EPPS) > Pb^{2+}, Mg^{2+}, Ca^{2+} > Cd^{2+} (Tris) > Sr^{2+}, $Ba^{2+} \gg Zn^{2+}$, Co^{2+}.

The rate of cleavage, k_2, versus [Mg^{2+}], [Ca^{2+}], or [Mn^{2+}] was examined under multiple-turnover conditions (Figure 4). The data for Mg^{2+} have been reported previously (*5*) and are included here for comparison. Multiple-turnover conditions were employed to allow a more facile measurement of k_2 when $k_2 > 1$ min^{-1}; single-turnover experiments would require very short sample times that could not be achieved by manual pipetting. A saturating concentration of S was used in these experiments so that k_2 was rate-determining. The DNA enzyme exhibited comparable levels of activity in the presence of a given concentration of either Ca^{2+} or Mg^{2+}. The catalytic rate was half-maximal in the presence of either ~180 mM Mg^{2+} or ~60 mM Ca^{2+}. For both of these metals, the apparent maximal rate of cleavage was ~5 min^{-1}. In contrast, half-maximal activity was obtained in the presence of only 2.6 mM Mn^{2+}, with an apparent maximal rate of Mn^{2+}-dependent cleavage of >10 min^{-1}. Values obtained in the presence of Mn^{2+}, especially at high concentrations, may be underestimated due to oxidation of Mn^{2+} at pH 7.5.

The pH dependence of the 10-23 DNA enzyme was studied in the presence of 10 mM Ca^{2+} at 37 °C (Figure 5). As above, the reactions were carried out under steady-state conditions in the presence of saturating [S] so that $k_{obs} = k_{cat} = k_2$. Three different buffers were employed in an overlapping manner to span a pH range from 6.1 to 9.7. The log of k_{cat} increased linearly with a slope of 0.94 as the pH increased from 6.5 to 8.5. This log-linear relationship did not hold either below pH 6.5 or above pH 8.5, indicating that under these conditions k_2 may not be rate-determining for the catalytic cycle or that k_2 is reduced due to titration of groups within the active site of the enzyme, as has been observed for the group I ribozyme (*11*).

The rate of substrate cleavage by the 10-23 DNA enzyme, k_2, is influenced by both divalent metal cations and pH. These observations support the hypothesis that the chemical mechanism of the enzyme involves a metal-assisted deprotonation event as part of the rate-limiting step of substrate cleavage. According to this hypothesis, the enzyme utilizes the metal to facilitate deprotonation of the 2′-hydroxyl group of the

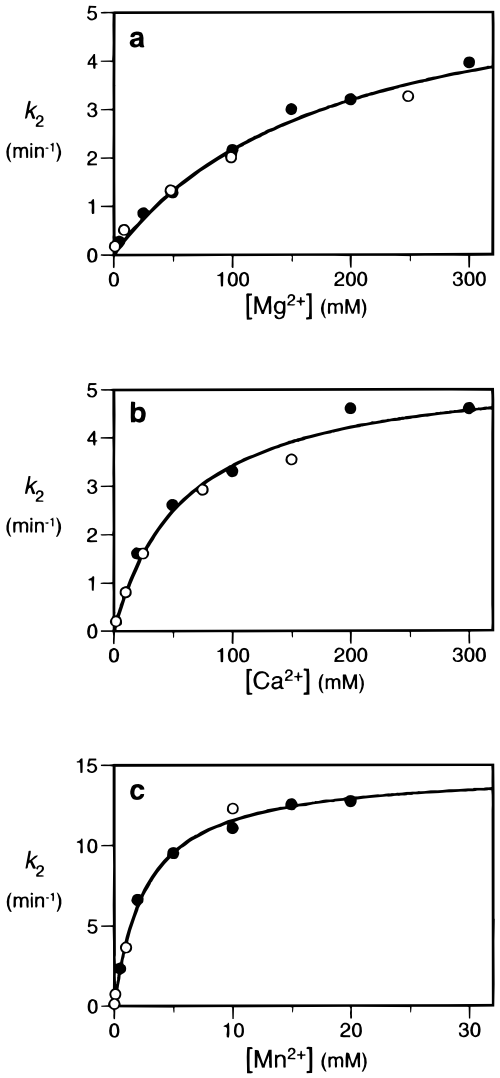

FIGURE 4: Dependence of the rate of substrate cleavage on the concentration of divalent metal cation. Reactions were carried out in the presence of either (a) Mg^{2+}, (b) Ca^{2+}, or (c) Mn^{2+}, together with 150 mM NaCl and 50 mM EPPS (pH 7.5) at 37 °C. Open and closed symbols correspond to independent experiments. The best-fit curves are based on the equation $k_2 = k_{max}[M^{2+}]/([M^{2+}] + K_d)$, where k_{max} is k_2 in the presence of saturating divalent metal cation and K_d is the apparent dissociation constant for the divalent metal cation.

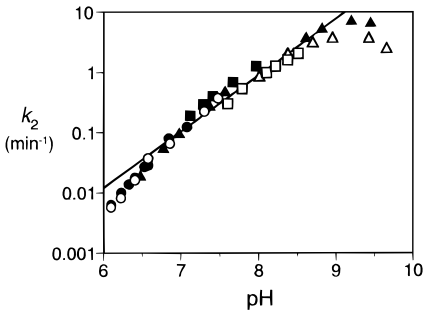

FIGURE 5: Dependence of the rate of substrate cleavage on pH. Reactions were carried out in the presence of 10 mM $CaCl_2$, 150 mM NaCl, and a 50 mM concentration of either PIPES (circles), EPPS (squares), or bis-Tris propane (triangles) at 37 °C. Open and closed symbols correspond to independent experiments. The best-fit line corresponds to data for pH 6.5−8.5 and has a slope of 0.94.

substrate that is located adjacent to the cleavage site (see Discussion). If this hypothesis is correct, then the chemical step of catalysis is rate-limiting for the conversion of E·S to E·P1·P2, and k_2 reflects the rate of the chemical step.

Comparison of Forward and Reverse Reaction Rates. Cleavage of an RNA substrate by the 10-23 DNA enzyme proceeded to near completion under conditions in which the substrate was present at high concentration and in excess over enzyme (data not shown). Assuming that under these conditions the concentration of products at equilibrium was sufficient to saturate the enzyme, this indicates that the rate of the forward reaction, cleavage, substantially exceeds the rate of the reverse reaction, ligation. The rate of the reverse reaction, k_{-2}, was measured by examining the ligation of the two products P1 and P2 to form the full-length substrate. Sufficient concentrations of E and P2 were used to ensure that all E was bound by P2 and that all 5′-^{32}P-labeled P1 was engaged in an E·P1·P2 complex. Under these conditions, the conversion of E·P1·P2 to E·S was monitored by the formation of a small but easily measurable amount of [5′-^{32}P]S. The reaction reached equilibrium with 0.0022 fraction ligated, with an observed rate of approach to equilibrium of 0.19 min^{-1}. Increasing the concentration of both E and P2 by 4-fold did not affect this result, indicating that saturation had been achieved. The observed rate of approach to equilibrium beginning with the two cleavage products reflects the sum of the rates of the forward and reverse reactions: $k_{obs} = k_2 + k_{-2} = 0.19$ min^{-1}. The rate of the forward reaction, k_2, under the same reaction conditions is 0.18 min^{-1}. Thus, k_{-2} is very slow relative to k_2.

An accurate estimate of the value of k_{-2} can be derived from the internal equilibrium constant, $K_{eq}^{int} = [E·P1·P2]/[E·S]$, which is equivalent to the inverse of the fraction ligated at equilibrium: $K_{eq}^{int} = 1/0.0022 = 450$. Because $K_{eq}^{int} = k_2/k_{-2}$, and $k_2 = 0.18$ min^{-1}, the rate of the reverse reaction, k_{-2}, is ∼0.0004 min^{-1}. This is consistent with the measured value for k_{obs} of 0.19 min^{-1}, indicating that the rate of approach to equilibrium involves only k_2 and k_{-2}. In summary, the 10-23 DNA enzyme exhibits a strong preference for the catalysis of cleavage over ligation under simulated physiological conditions.

Evaluation of Enzyme−Substrate Dissociation and Association Rates. Pulse−chase experiments were used to compare the rate of enzyme−substrate dissociation, k_{-1}, to the rate of substrate cleavage, k_2, to establish an upper limit for k_{-1}. A saturating concentration of E was first allowed to bind a trace amount of [5′-^{32}P]S for a period, t_1, of 30 s. Then a large amount of unlabeled S was added to the mixture to initiate the chase period, t_2, during which dissociation of [5′-^{32}P]S from E was essentially irreversible. An otherwise identical reaction, but without the chase, was carried out in parallel. Removal and quenching of samples from the two reaction mixtures at various times allowed the final extent of cleavage to be determined in each case. The extent of cleavage was the same for the two reactions, indicating that the rate constant for substrate cleavage, k_2, is much greater than the rate constant for substrate dissociation, k_{-1}. This sets an upper limit for k_{-1} that is at least 10-fold slower than k_2, so that $k_{-1} < 0.018$ min^{-1}.

Because $k_{cat} = k_2 \gg k_{-1}$, the second-order rate constant for cleavage, k_{cat}/K_M, reduces from $k_1k_2/(k_{-1} + k_2)$ to simply k_1. Thus, catalytic efficiency, k_{cat}/K_M, is expected to be approximately equal to the rate constant for enzyme−substrate association. A series of pulse−chase experiments

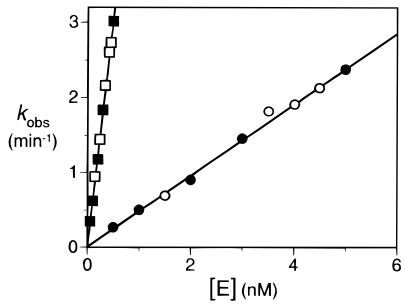

FIGURE 6: Rate of association of the 10-23 DNA enzyme and an RNA substrate. Pulse−chase experiments were used to measure k_1 and k_{-1}, determined by the slope and *y*-intercept, respectively, of lines fit to data obtained in the presence of either 2 (circles) or 100 (squares) mM Mg^{2+}. k_{obs} corresponds to the rate of approach to equilibrium for enzyme−substrate association. Open and closed symbols correspond to independent experiments.

Table 1: Second-Order Rate Constants for Interaction with a 17mer RNA Substrate[a]

rate constant (M^{-1} min^{-1})	2 mM Mg^{2+}	100 mM Mg^{2+}
k_{cat}/K_m, DNA enzyme (8+8)	3.2×10^8	4.9×10^9
k_{assoc}, DNA enzyme (8+8)	4.7×10^8	6.0×10^9
k_{assoc}, 17mer DNA (d17)	6.6×10^8	6.4×10^9
k_{assoc}, 16mer DNA (d16)	6.6×10^8	7.1×10^9
k_{assoc}, 17mer RNA (r17)	9.0×10^8	nd
k_{assoc}, 16mer RNA (r16)	8.8×10^8	nd

[a] Reaction conditions: 2 or 100 mM $MgCl_2$, 150 mM NaCl, 50 mM EPPS (pH 7.5), 37 °C.

were carried out to test this hypothesis, measuring k_1 in the presence of either 2 or 100 mM Mg^{2+} (Figure 3a). Varying concentrations of E were first allowed to bind to a trace amount of [5′-^{32}P]S for varying times, t_1, ranging from 0 to 10 min. Then a large excess of unlabeled substrate was added to the reaction mixture, effectively preventing any further binding of [5′-^{32}P]S. Following the chase, the reactions were allowed to proceed for a period, t_2, that was sufficient to ensure complete cleavage of any [5′-^{32}P]S that had been bound by E during t_1. Measurement of the amount of cleavage as a function of t_1 provided a value for k_{obs} for each [E].

In these pulse−chase experiments, k_{obs} represents the rate of approach to equilibrium for formation of the E·S complex, which reflects the sum of the rate constants for association and dissociation: $k_{obs} = k_1[E] + k_{-1}$. A plot of k_{obs} vs [E] (Figure 6) provides a best-fit line with slope equal to k_1 and *y*-intercept equal to k_{-1}. Values for k_1 obtained in the presence of either 2 or 100 mM Mg^{2+} were in close agreement with values for the second-order rate constant, k_{cat}/K_M, obtained under the same reaction conditions (Table 1). Thus, k_{cat}/K_M is determined primarily by k_1, the rate of enzyme−substrate association. The value obtained for the rate of enzyme−substrate dissociation, k_{-1}, from pulse−chase experiments carried out in the presence of 2 mM Mg^{2+} is <0.03 min^{-1}, consistent with the upper limit for k_{-1} of 0.018 min^{-1} that was obtained in experiments comparing k_{-1} and k_2, as described above.

Association Rates of Complementary Oligonucleotides. The rate of association of the 10-23 DNA enzyme and an RNA substrate was compared to the rate of formation of a corresponding DNA−RNA or RNA−RNA duplex. This was done in order to assess the possible contribution of the 15-nucleotide catalytic core of the enzyme, the single bulged purine residue of the substrate, and the heteroduplex nature of the enzyme−substrate complex to the rate of enzyme−substrate association. The rate was determined for association of the substrate with four different complementary oligonucleotides: d17, a 17mer DNA that is perfectly complementary to S; d16, a 16mer DNA that lacks a residue opposite the bulged A of the substrate and thus more closely mimics the E·S complex; r17, the RNA analogue of d17; and r16, the RNA analogue of d16.

A series of pulse−chase experiments were carried out to measure k_{assoc} for each substrate−oligonucleotide pair in the presence of either 2 or 100 mM Mg^{2+} (Figure 3b). Varying concentrations of complementary oligonucleotide were first allowed to bind to a trace amount of [5′-^{32}P]S for varying times, t_1. Then a large excess of E was added to the reaction mixture, effectively preventing any further binding of [5′-^{32}P]S. Following the chase, the reactions were allowed to proceed for a time, t_2, that was sufficient to ensure complete cleavage of any [5′-^{32}P]S that had not been bound by the complementary oligonucleotide during t_1. Measurement of the amount of cleavage as a function of t_1 provided a value for k_{obs} for each concentration of oligonucleotide. In this case, k_{obs} represents the rate of approach to equilibrium for formation of the substrate−oligonucleotide complex, reflecting the sum of the rate constants for association and dissociation: $k_{obs} = k_{assoc}$[oligonucleotide] + k_{dissoc}. A plot of k_{obs} versus [oligonucleotide] provided a best-fit line with slope equal to k_{assoc} and *y*-intercept equal to k_{dissoc}.

The k_{assoc} values for both d16 and d17 (Table 1) are only slightly higher than the k_1 value for the DNA enzyme with the same RNA. Thus, the rate of enzyme−substrate association is nearly identical to the rate of formation of the comparable DNA−RNA heteroduplex. The k_{assoc} values for the two complementary RNA oligonucleotides, r17 and r16, are slightly higher than those for d17 and d16, when measured in the presence of 2 mM Mg^{2+} (Table 1). This suggests that DNA−RNA heteroduplexes do not form at a faster rate than the corresponding RNA−RNA homoduplexes and, therefore, that the rate of association of the 10-23 DNA enzyme with an RNA substrate is not significantly affected by the heteroduplex nature of the enzyme−substrate complex.

To exclude the possibility that the RNA substrate employed in this study is unusual with respect to its duplex association rate, three additional substrates with very different sequences were examined (see Materials and Methods). Each substrate was allowed to hybridize with a complemetary DNA before the chase was initiated with the corresponding DNA enzyme. In all cases, the association rate in the presence of 2 mM Mg^{2+} was $\sim 2 \times 10^8$ M^{-1} min^{-1} (data not shown).

Analysis of Substrate Sequence Specificity. The ability of the 10-23 DNA enzyme to discriminate between matched and mismatched substrates was investigated, employing the 7+7 version of the enzyme under multiple-turnover conditions. Values for k_{cat} and K_M were determined for a series of mismatched substrates, each containing a single conservative nucleotide substitution (Figure 7). All of the mismatched RNAs were cleaved less efficiently than the fully matched substrate. In some cases, the reduction in catalytic efficiency

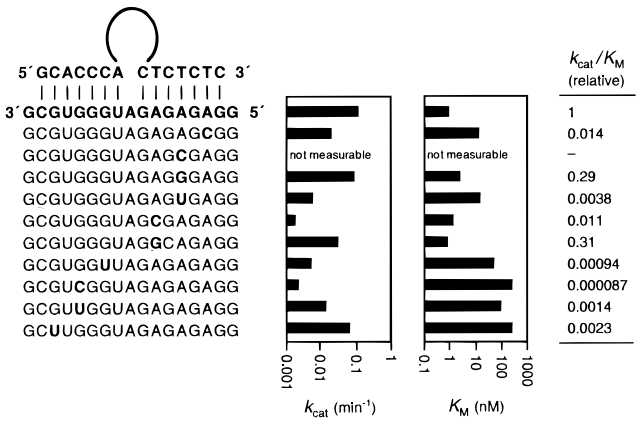

FIGURE 7: Substrate sequence specificity of the 10-23 DNA enzyme. Values for k_{cat} and K_M were determined for cleavage of substrates with a single base mismatch, as indicated in boldface type below the fully matched sequence. Relative values for k_{cat}/K_M were determined by comparison to cleavage of the fully matched substrate; a low relative value corresponds to high specificity in discriminating against the mismatched substrate. k_{cat}/K_M for cleavage of the fully matched substrate by the 7+7 DNA enzyme was 1.2×10^8 M^{-1} min^{-1}. Reaction conditions: 2 mM $MgCl_2$, 150 mM NaCl, 50 mM EPPS (pH 7.5), 37 °C.

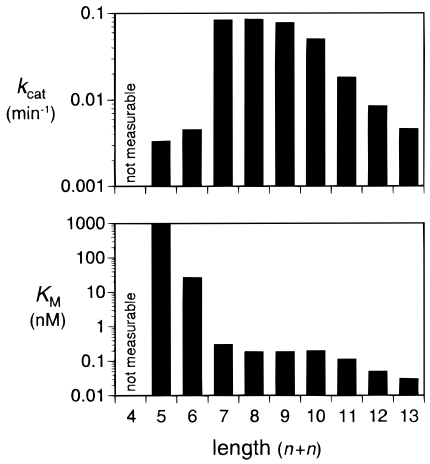

FIGURE 8: Effects of varying the length of the substrate-recognition domains. Values for k_{cat} and K_M were obtained for DNA enzymes with recognition domains of equal length, ranging from 4+4 to 13+13. Reaction conditions: 2 mM $MgCl_2$, 150 mM NaCl, 50 mM EPPS (pH 7.5), 37 °C.

was due largely to a reduction in k_{cat}, reflecting a decrease in k_2, while in other cases it was due largely to an increase in K_M, indicating reduced substrate binding affinity. Mismatches that involved the formation of a single wobble pair resulted in a relatively modest reduction in catalytic efficiency (~3-fold). All other mismatches, which involved a pyrimidine−pyrimidine opposition, resulted in a more dramatic reduction (71-fold to >12 000-fold).

Variation of Substrate-Recognition Domain Length. Previous experiments indicated that small changes in the length of the substrate-recognition domains could result in substantial alteration of the catalytic efficiency of the 10-23 DNA enzyme (*5*). In addition, because the two cleavage products are bound by these same recognition domains, it is expected that very long domains would result in slow product release and, therefore, slow catalytic turnover. A systematic study of the effect of substrate-recognition domain length on catalysis was carried out by measuring k_{cat} and K_M under steady-state, multiple-turnover conditions for a series of DNA enzymes with recognition domains of symmetrical length ranging from 4+4 to 13+13 (Figure 8). Each enzyme was directed to cleave the same 27mer RNA substrate, corresponding in sequence to the region surrounding the start codon of HIV-1 *gag-pol* mRNA. Catalytic efficiency rose sharply as the length of the substrate-recognition domains increased from 4+4 to 7+7. Enzymes with recognition domains ranging in length from 7+7 to 13+13 exhibited similar catalytic efficiencies, reflecting the fact that k_{cat}/K_M for these enzymes is limited by k_1, which is approximately the same in all cases.

As the substrate-recognition domains were lengthened beyond 9+9, there was a progressive decrease in k_{cat} that was thought to reflect a change in the rate-determining step of the catalytic cycle from chemistry to product release. To verify this possibility, single-turnover experiments were carried out under the same reaction conditions to measure the rate of substrate cleavage, k_2, for both the 8+8 and 13+13 enzymes. These enzymes exhibited the same value for k_2 of 0.11 min^{-1}, even though the 13+13 enzyme had an 18-fold lower value for k_{cat} under multiple-turnover conditions. Furthermore, experimentally determined values for k_{cat} under multiple-turnover conditions were consistent with calculated rates of product release, assuming that the enzyme−product complex behaves as two independent DNA−RNA heteroduplexes (see Discussion).

Compositional Requirements of the Enzyme and Substrate. The sequence requirements of the catalytic core of the 10-23 DNA enzyme were investigated previously by generating a large population of enzyme variants in which random mutations were introduced throughout the core and then subjecting the population to repeated rounds of selective amplification based on RNA-cleavage activity (*5*). The activity of the enzyme was found to be almost completely intolerant of sequence changes within the catalytic core. The sole exception was a T→C or T→A change at the eighth nucleotide position that reduced, but did not eliminate, catalytic activity. Based on these observations, a "disabled" DNA enzyme was constructed by introducing a single G→C change at the sixth position of the catalytic core (changing the core sequence to 5′-GGCTACCTACAACGA-3′, mutation underlined). This single substitution was found to abolish enzyme activity, providing a control molecule that is inactive but retains Watson−Crick complementarity to the RNA substrate.

As reported previously, the rate of cleavage by the 10-23 DNA enzyme is largely independent of the sequence of the RNA substrate except for the two substrate nucleotides immediately surrounding the cleavage site (*5*). The enzyme prefers to cleave an RNA phosphoester located between an unpaired purine and paired pyrimidine residue. Sequences of the form 5′-RU-3′ (R = A or G) are cleaved most rapidly. To more completely define the sequence preference of the DNA enzyme with respect to the unpaired substrate nucleotide, five different substrates were constructed, each containing one of the four standard nucleotides or no nucleotide at the single unpaired position, with the remainder of the sequence being constant. Measurement of k_{cat} and K_M under multiple-turnover conditions (Table 2) revealed that the enzyme prefers to cleave after G and, to a slightly lesser extent, after A. Cleavage after U or no unpaired residue

Table 2: Effects of Varying the Unpaired Residue of the RNA Substrate[a]

substrate	k_{cat} (min^{-1})	K_M (nM)
5′-GGAGAGAG**A**UGGGUGCG-3′	0.11	0.89
5′-GGAGAGAG**C**UGGGUGCG-3′	nm[b]	nm
5′-GGAGAGAG**G**UGGGUGCG-3′	0.39	1.4
5′-GGAGAGAG**U**UGGGUGCG-3′	0.027	0.41
5′-GGAGAGAG-UGGGUGCG-3′	0.050	0.77

[a] The unpaired substrate nucleotide position is shown in boldface type. Results were obtained with the 7+7 DNA enzyme. Reaction conditions: 2 mM $MgCl_2$, 150 mM NaCl, 50 mM EPPS (pH 7.5), 37 °C. [b] Not measurable.

was much less efficient, and cleavage after C was undetectable.

DISCUSSION

These investigations into the catalytic behavior of the 10-23 DNA enzyme have provided an enhanced understanding of its mechanism and, ultimately, the scope of its utility. The enzyme exhibits properties that make it a promising candidate for use as a synthetic endoribonuclease, both in the laboratory and in biological systems. Its small size, all-DNA composition, target sequence versatility, and high catalytic efficiency are among the most important of these properties. The following discussion highlights mechanistic features of the DNA enzyme that are relevant to its potential applicability.

Chemical Mechanism of the DNA Enzyme. The 10-23 DNA enzyme was selected on the basis of its ability to cleave RNA in the presence of Mg^{2+}. Not surprisingly, enzyme activity is observed only in the presence of Mg^{2+} (*5*) or one of several other divalent metal cations, including Ca^{2+}, Mn^{2+}, Pb^{2+}, and, to a lesser extent, Cd^{2+}, Sr^{2+}, and Ba^{2+}. In this regard, the enzyme behaves similarly to the hammerhead ribozyme, which also is active in the presence of various divalent metal cations (*12*). These metals might help to stabilize the transition state of the reaction and/or assist in folding of the enzyme into its active conformation.

The order of activity for the various metals corresponds roughly to the inverse order of the pK_a values of the respective metal hydrates. This might be taken as evidence to support a particular metal-assisted reaction mechanism, although interpretation of this observation is problematic for two reasons. First, the correlation does not hold for all metals. For example, the catalytic rate of the enzyme is approximately the same in the presence of saturating concentrations of either Mg^{2+} or Ca^{2+} (Figure 4), despite the difference of 1.5 units in the pK_a of the corresponding metal hydrate (*13*). On the other hand, the catalytic rate in the presence of saturating Mn^{2+} is ~3-fold higher than in the presence of saturating Mg^{2+}, which more closely parallels the difference in the pK_a values of the respective metal hydrates. Second, the apparent binding affinities of the various metals are quite different, suggesting that they might bind to the enzyme in a different manner. For example, the enzyme appears to bind Ca^{2+} and especially Mn^{2+} more tightly than it binds Mg^{2+}. Catalytic activity is half-maximal in the presence of either 180 mM Mg^{2+}, 60 mM Ca^{2+}, or 2.6 mM Mn^{2+} (Figure 4). Even slight differences in the occupancy or positioning of the various metals within the enzyme may lead to large differences in the catalytic rate, making comparisons extremely difficult.

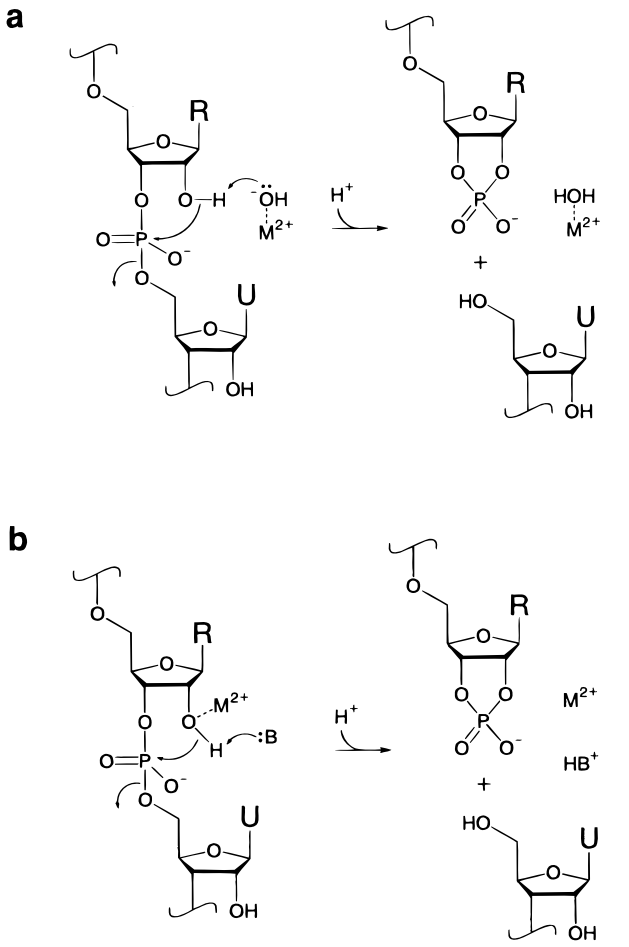

FIGURE 9: Two hypothetical chemical mechanisms for catalysis of RNA cleavage by the 10-23 DNA enzyme. (a) Mechanism involving a divalent metal hydroxide that functions as a general base. (b) Mechanism involving a divalent metal cation that functions as a Lewis acid.

As reported previously (*5*), RNA cleavage catalyzed by the 10-23 DNA enzyme results in an upstream fragment terminating in a 2′,3′-cyclic phosphate and a downstream fragment terminating in a 5′-hydroxyl. This, together with the divalent metal cation dependence of the enzyme, can be taken as evidence to support a chemical mechanism involving metal-assisted deprotonation of the 2′-hydroxyl located adjacent to the cleavage site. This would produce a nucleophilic 2′-oxyanion that attacks the adjacent phosphorus, giving rise to the observed cleavage products. The metal may participate in the chemical mechanism of the DNA enzyme either as a metal hydroxide that functions as a general base to assist in deprotonation of the 2′-hydroxyl (Figure 9a) or as a Lewis acid that coordinates directly to the 2′-hydroxyl and enhances its acidity (Figure 9b). The metal might also play a purely structural role, helping to organize the enzyme into its active conformation.

Regardless of the precise role of the metal, if deprotonation of the 2′-hydroxyl is part of the rate-limiting step of cleavage, then the catalytic rate would be expected to increase log-linearly with increasing pH. This is the case over a pH range of 6.5−8.5 in the presence of 10 mM Ca^{2+} (Figure 5). Similar results were obtained with various concentrations of other divalent metal cations (data not shown). The log-linear increase with a slope of ~1 indicates that a single deprotonation event occurs during the rate-limiting step of the

reaction (*14*). It is possible that this deprotonation event involves a conformational change of the enzyme−substrate complex prior to the chemical step, but it more likely corresponds to deprotonation of the 2′-hydroxyl that results in cleavage of the adjacent phosphoester. Analogous deprotonation events are thought to be involved in the mechanism of several small RNA-cleaving RNA enzymes, including the hammerhead and hairpin ribozymes (for reviews, see *2, 15, 16*).

Preference for Cleavage Over Ligation. The 10-23 DNA enzyme, in the presence of a divalent metal cation, stabilizes the transition state leading to the forward cleavage reaction. Thus, the enzyme must also accelerate the reverse reaction that results in ligation of the two cleavage products (*14*). To compare the rates of cleavage and ligation, the internal equilibrium constant, K_{eq}^{int}, was determined. This value is equal to the relative rates of the forward and reverse reactions, k_2/k_{-2}. Under simulated physiological conditions, K_{eq}^{int} is 450, indicating a strong preference for cleavage over ligation. This preference would not be expected on the basis of enthalpy changes because the 2′,3′-cyclic phosphate is strained and therefore enthalpically unfavorable relative to the 3′,5′-phosphodiester (*17*). It thus appears that the enzyme compensates for the enthalpy loss by an even larger entropic gain, presumably due to loss of structural integrity of the enzyme−product complex following substrate cleavage. After cleavage, the reactive termini of the two products may not be held in sufficiently close proximity to facilitate their rapid ligation.

The preference for cleavage over ligation by the DNA enzyme is nearly identical to that observed for the hammerhead ribozyme under similar reaction conditions (*18*). The hairpin ribozyme, in contrast, has a rate of product ligation that is ∼10-fold faster than the rate of substrate cleavage (*19*). These preferences may be rationalized by considering the selection pressure that applied to each catalyst during its evolutionary development. The 10-23 DNA enzyme was selected in vitro based on its ability to cleave a tethered oligoribonucleotide and thus become detached from a solid support (*5*). The hammerhead ribozyme was evolved in nature to operate in a similar self-cleavage format, converting the multimeric product of rolling-circle RNA replication to monomeric genomic RNAs (*20, 21*). In contrast, the hairpin ribozyme was evolved both to cleave multimeric genomic RNA to monomeric units and to ligate those monomers to form covalently closed circles (*22, 23*). As a result, the hairpin ribozyme was selected on the basis of both cleavage and ligation activity, and thus is expected to have a value for K_{eq}^{int} close to unity.

Rate of Catalytic Turnover. The rate of catalytic turnover of an enzyme in the presence of saturating substrate, k_{cat}, is an important measure of its catalytic activity. Maximizing the turnover rate of the 10-23 DNA enzyme requires that all other steps of the catalytic cycle be faster than the rate of cleavage, k_2, in the presence of a saturating concentration of substrate. In terms of the minimal kinetic scheme presented in Figure 2, this requires that the rate of product release, k_3, be faster than k_2. This is true for the DNA enzymes that contained substrate-recognition domains of less than 10 nucleotides each (Figure 8). However, for DNA enzymes with longer recognition domains, k_3 was less than k_2, so that k_{cat} was determined by the rate of product release.

Even though the RNA substrate employed in this study had a high GC content, product release did not become rate-limiting unless the recognition domains were quite long. For substrates with lower GC content, the recognition domains likely could be made even longer without impairing catalytic turnover. In contrast, the substrate-recognition domains of the hammerhead ribozyme must be kept significantly shorter to prevent product release from becoming rate limiting (*24*). This may be due in part to the slower rate of dissociation of RNA−RNA homoduplexes compared to DNA−RNA heteroduplexes of the same sequence (*25*).

The DNA enzyme possessing substrate-recognition domains of eight nucleotides each exhibits a k_{cat} that varies substantially depending upon the reaction conditions. Changes in the pH, choice of divalent metal cation, and divalent metal cation concentration all affect the rate of substrate cleavage, and therefore k_{cat}. In the presence of 2 mM Mg^{2+} and 150 mM monovalent cation at pH 7.5 and 37 °C, conditions that approximate those of a living cell, k_{cat} is ∼0.1 min^{-1}. Under less physiological conditions, such as higher divalent cation concentration and/or higher pH, k_{cat} can exceed 10 min^{-1}.

Catalytic Efficiency of the DNA Enzyme. RNA-cleaving RNA enzymes that bind their substrate through long stretches of Watson−Crick pairing generally perform substrate cleavage and product release at rates that are much faster than the rate of enzyme−substrate dissociation (*8*−*10, 19*). This is due to the high thermodynamic stability of the enzyme−substrate complex. As a result, nearly every substrate binding event results in substrate cleavage. For these enzymes, catalytic efficiency (k_{cat}/K_M) is limited by the rate of enzyme−substrate association. Mathematically, this results from the fact that if $k_{cat} = k_2 \gg k_{-1}$, then the second-order rate constant, $k_{cat}/K_M = k_1k_2/(k_{-1} + k_2)$, reduces to k_1.

Because RNA-cleaving RNA enzymes bind their substrates through Watson−Crick pairing, k_1 may be at least partially determined by the rate of RNA−RNA hybridization. A reasonable expectation, based on the similar mode of substrate binding by the 10-23 DNA enzyme, is that it too is limited by the rate of enzyme−substrate association, and therefore by the rate of DNA−RNA hybridization. To test this hypothesis, it was first necessary to confirm that $k_{cat} \gg k_{-1}$ for the DNA enzyme. Using pulse−chase experiments, k_2 was found to be at least 10-fold greater than k_{-1}. Next, pulse−chase experiments were used to measure k_1 for the DNA enzyme (Figure 6). In the presence of 2 mM Mg^{2+}, k_1 was 4.6×10^8 M^{-1} min^{-1}, which agrees closely with the value for k_{cat}/K_M of 3.2×10^8 M^{-1} min^{-1}, measured under the same reaction conditions. In the presence of 100 mM Mg^{2+}, k_1 was 6.1×10^9 M^{-1} min^{-1}, and k_{cat}/K_M was 4.9×10^9 M^{-1} min^{-1}, again in close agreement (Table 1).

The values for k_1 and k_{cat}/K_M for the 10-23 DNA enzyme are more than an order of magnitude higher than those for the hammerhead and group I ribozymes, measured under similar reaction conditions (*9, 10, 26*). Conceivably, these differences could be explained by differences in the relative rates of formation of DNA−RNA versus RNA−RNA duplexes. There is one report in the literature indicating little difference in the rate of formation of DNA−RNA and RNA−RNA duplexes of the same sequence (*25*). However, that study was conducted with only one, relatively short (7mer) oligonucleotide sequence. To confirm those results, the present study included measurements of the association

rate of the RNA substrate with either a complementary DNA or a complementary RNA oligonucleotide. This was accomplished using a novel pulse−chase technique in which the DNA enzyme served as the "chase", cleaving any substrate that had not become associated with the complementary oligonucleotide during the initial "pulse" period. The rate of formation of the DNA−RNA heteroduplex was nearly identical to that of the enzyme−substrate complex. Formation of a comparable RNA−RNA homoduplex was only slightly faster. These data were unaffected by the presence of a single unpaired purine nucleotide within the substrate strand.

It is possible that the particular substrate employed in this study is unusual with respect to its rate of duplex formation, resulting in unusually high values for k_1. To exclude this possibility, the same pulse−chase technique was used to measure the rates of duplex formation for three other RNA substrates having very different sequences. The association of each of these substrates with a complementary oligodeoxynucleotide occurred at a rate similar to that observed for the standard RNA substrate.

These experiments demonstrate that DNA−RNA hybridization is not inherently faster than RNA−RNA hybridization and that the RNA substrate employed in this study is typical with respect to its rate of duplex formation. Furthermore, the DNA enzyme is operating close to the limit imposed by the rate of duplex formation. The faster rate of enzyme−substrate association for the 10-23 DNA enzyme as compared to various RNA-cleaving RNA enzymes may be due to a lower propensity of the DNA enzyme to adopt alternative structures that reduce the rate of substrate binding.

The DNA enzyme exhibits a >10-fold enhanced rate of substrate binding in the presence of 100 mM Mg^{2+} as compared to 2 mM Mg^{2+}. This dependence of association rate on the concentration of divalent cation also has been observed for the association of complementary oligonucleotides (*27, 28*) and ribozyme−substrate complexes (*26*). This behavior can be explained by the counterion−condensation model for nucleic acid helix formation (*29*−*31*), in which negative charges on the oligonucleotides are shielded by the divalent cation to allow more rapid strand interaction. Low molecular weight compounds, such as cetyltrimethylammonium bromide, and various cellular proteins also can enhance the rate of association of complementary nucleic acids (*32*−*34*).

Catalytic efficiency is optimal when the substrate-recognition domains are sufficiently long that k_{cat}/K_M is determined by the rate of enzyme−substrate association, k_1. This occurs when the rate of substrate cleavage, k_2, substantially exceeds the rate of enzyme−substrate dissociation, k_{-1}. For a catalytically "perfect" enzyme (*35*), k_1 is equivalent to the rate of diffusional encounter of the enzyme and substrate. In contrast, k_1 for the DNA enzyme is expected to be limited by the rate of duplex formation. This limits the maximal catalytic efficiency for such an enzyme to 10^8−10^{10} M^{-1} min^{-1}, depending on the cation concentration, thus lowering the criterion for enzymatic "perfection". The 10-23 DNA enzyme, with substrate-recognition domains of at least seven nucleotides each, meets this lowered criterion. k_{-1} for these enzymes is slow relative to both k_2 and the rate of product release, k_3. Therefore, k_{cat}/K_M is equal to k_1, which in turn is equal to the rate of DNA−RNA heteroduplex formation. When the substrate-recognition domains were less than seven nucleotides each, the enzyme exhibited lower values for k_1 and/or higher values for k_{-1}, so that k_{cat}/K_M was less than the rate of duplex formation. When the domains were lengthened beyond 10 nucleotides each, K_M was reduced, but k_{cat} also was lower due to rate-limiting product release, so that k_{cat}/K_M remained nearly unchanged (Figure 8).

Substrate Sequence Discrimination by the DNA Enzyme. The specificity of an enzyme, that is, the degree to which it can discriminate between two substrates, can be described quantitatively by the ratio of the catalytic efficiencies of the respective enzyme-catalyzed reactions (*14*). Specificity values for the DNA enzyme with recognition domains of seven nucleotides each ranged from 3 to $>1.2 \times 10^4$, comparing a matched substrate to substrates with a single base mismatch (Figure 7). Not surprisingly, specificity values were lowest for substrates that contained a single G·T or U·G wobble mismatch, indicating little discrimination against these substrates. In general, mismatches located proximal to the cleavage site resulted in a greater decrease in k_{cat} compared to those located more distally. This is presumably due to greater distortion of the active site for mismatches that occur closer to the scissile bond. In this regard, the 10-23 DNA enzyme behaves similarly to other nucleic acid enzymes (*36*−*39*) and contrasts with traditional antisense agents that derive their specificity largely as a result of differential binding affinity.

Substrate sequence specificity for cleavage of an RNA substrate by a nucleic acid enzyme is affected by the length of the substrate-recognition domains. To achieve high sequence specificity, the domains must be short enough to render them sensitive to base mismatches. This occurs when the rate of enzyme−substrate dissociation for a mismatched substrate is greater than the rate of substrate cleavage, that is, when $k_{-1} > k_2$ (*40, 41*). For example, the DNA enzyme with recognition domains of seven nucleotides each exhibits 20−50-fold enhanced sensitivity to single base mismatches compared to the enzyme with recognition domains of eight nucleotides each (data not shown). This indicates that k_{-1} is much closer to k_2 for the shorter enzyme. These data are consistent with the calculated values for k_{-1} for the two enzymes, based upon the predicted thermodynamic stability of the corresponding enzyme−substrate complexes (*42*). Assuming a helix-initiation penalty for each component duplex of the enzyme−substrate complex and applying the experimentally determined value for k_1 of 4.6×10^8 M^{-1} min^{-1}, the predicted values for k_{-1} are 3×10^{-3} min^{-1} and 2×10^{-6} min^{-1} for the 7+7 and 8+8 enzymes, respectively. For applications where sequence specificity is important, the enhanced specificity of the shorter enzyme may outweigh its slightly reduced catalytic efficiency. It would be difficult to justify the use of an enzyme with recognition domains shorter than 7+7, however, despite the further enhancement of sequence specificity, because such an enzyme would exhibit severely reduced catalytic efficiency.

Substrate sequence selectivity, the degree to which the enzyme can recognize an RNA target sequence that is unique among accessible RNAs, also is affected by the length of the recognition domains. It is estimated that ~14 nucleotides are necessary to define a unique RNA sequence within human cells. High sequence selectivity in this context therefore requires that the recognition domains of the enzyme

together comprise at least 14 nucleotides. Of course an increase in sequence selectivity is meaningless if it leads to a decrease in sequence specificity (*40*). Fortunately, the recognition domain lengths that are required for the 10-23 DNA enzyme to achieve high sequence specificity also allow high sequence selectivity. Among the dozens of substrate sequences that have been targeted by the 10-23 DNA enzyme (data not shown), the combined length of the optimized recognition domains ranges from 14 to 20 nucleotides.

Substrate sequence specificity and selectivity can together be described by a "discrimination index", which is defined as the relative rates of targeted versus nontargeted RNA cleavage within a mixture of sequences (*40*). The inherently faster rate of dissociation of DNA−RNA heteroduplexes as compared to RNA−RNA homoduplexes (*25*), in addition to permitting faster product release, may allow the DNA enzyme to recognize longer RNA target sequences with high specificity compared to analogous RNA-cleaving RNA enzymes. Therefore, DNA enzymes may have an inherent advantage over RNA enzymes with respect to target discrimination.

Application of the DNA Enzyme. The 10-23 DNA enzyme is a potentially powerful tool for applications involving the sequence-specific cleavage of RNA. These include its use in vitro as an RNA restriction endonuclease and its use in biological systems as an agent for gene inactivation at the level of mRNA. Effective use of the DNA enzyme requires an understanding of several important biochemical issues, some that are unique to the enzyme and others that apply more generally to RNA-cleaving nucleic acid enzymes and antisense agents.

A critical factor in applying the DNA enzyme is the choice of a suitable cleavage site within the target RNA. The DNA enzyme can be made to cleave any RNA that contains a 5′-RY-3′ sequence surrounding the cleavage site, with the sequences 5′-GU-3′ and 5′-AU-3′ being cleaved most rapidly (*5*). A more complex issue is the requirement that the target site be accessible to the DNA enzyme within the folded structure of the RNA. Poor accessibility can result in a decreased rate of enzyme−substrate association and thus decreased catalytic efficiency (data not shown). For applications involving short RNAs, target site accessibility can be predicted using folding algorithms (*43, 44*). Full-length mRNAs and other structurally complex RNAs present a more difficult challenge in identifying accessible sites within a folded structure that typically is unknown. The problem of site accessibility within a long RNA has been extensively discussed in the antisense literature. Although several promising experimental approaches have been offered for identifying accessible sites (see, for example, *45*−*51*), the currently preferred method remains one of trial and error (*52*).

Optimal catalytic efficiency also requires that the DNA enzyme not adopt a stable self-structure that would prevent its substrate-recognition domains from being available to bind the substrate. Some sequences are unsuitable for use in the recognition domains of the enzyme because they would cause the domains to pair with themselves or with the catalytic core. Competing self-structure within the DNA enzyme has been found to result in an increased K_M and a corresponding decrease in catalytic efficiency (data not shown). Fortunately, the DNA enzyme is sufficiently small that problems with stable self-structure are easy to predict and therefore easy to avoid.

The optimal lengths of the two substrate-recognition domains with regard to the enzyme's catalytic efficiency, turnover rate, and substrate sequence specificity and selectivity are determined by the strength of the binding interaction between these domains and the RNA substrate. This in turn is determined by the base composition of the substrate. The RNA target sequence employed in this study had a high GC content and therefore required shorter substrate-recognition domains than would have been required for a more AU-rich substrate. This study employed enzymes with recognition domains of symmetrical length. This may not always be optimal, especially when there are substantial differences in the GC content of the two domains.

Conveniently, the substrate-recognition domains of the DNA enzyme bind the RNA substrate through simple Watson−Crick pairing so that the stability of these interactions is easy to predict. For a given target sequence, it is possible to estimate with good accuracy the optimal length of each substrate-recognition domain based on calculated duplex stabilities (*42*). If the results obtained in this study with the HIV-1 *gag-pol* substrate can be generalized, the predicted stability for each recognition-domain interaction (including a helix initiation penalty) should be −8 to −10 kcal mol^{-1}, depending on whether optimal substrate sequence specificity or optimal catalytic efficiency is deemed more important for the particular application (see above). Duplex stabilities in this range are well below what would result in rate-limiting product release. If reaction conditions are employed that differ substantially from those reported in this study, it may be necessary to adjust the length of the substrate-recognition domains accordingly. In the presence of higher concentrations of divalent metal cation, for example, where the rate of substrate cleavage is increased and the rate of product release is decreased, the optimal lengths of the substrate-recognition domains are likely to be shorter.

The 10-23 DNA enzyme can be used in vitro under a broad range of reaction conditions, varying the pH, divalent metal cation, and divalent metal cation concentration. These parameters affect both the rate of enzyme catalysis and the uncatalyzed rate of RNA cleavage. The preferred reaction condition will depend on the particular application. A convenient reaction condition that does not result in appreciable uncatalyzed RNA cleavage employs 10 mM Ca^{2+}, 50 mM EPPS (pH 7.5), and 40 μg/mL BSA at 37 °C. The enzyme described in the present study operates with a k_{cat} of 0.8 min^{-1} and K_M of 1 nM under these conditions.

Effective application of the DNA enzyme to biological systems requires that it significantly reduce the cellular concentration of a target RNA for a biologically relevant period of time, without causing cellular toxicity or other undesirable side effects. In this context, the DNA enzyme faces many of the same challenges that confront other nucleic-acid based gene-inactivation agents (for reviews, see *53*−*55*). Efficient cellular uptake, proper subcellular localization, resistance to nuclease degradation, and favorable pharmacokinetic properties are some of the key issues that will determine the efficacy of the DNA enzyme in vivo. Because the enzyme is composed of DNA, it will be susceptible to degradation by deoxyribonucleases unless steps

are taken to ensure its resistance. A wide variety of chemical modifications have been developed to stabilize traditional antisense agents against both endonucleolytic and exonucleolytic degradation (for reviews, see *53*, *56*, *57*). Many of these modifications can be incorporated into the 10-23 DNA enzyme to confer nuclease protection. Preferred modifications include attachment of an inverted (3′,3′-linked) thymidylate at the 3′ end of the enzyme, substitution of either phosphorothioate or 2′-*O*-methyl nucleotide analogues within the substrate-recognition domains, and substitution of phosphorothioate analogues at pyrimidine positions within the catalytic core. DNA enzymes that were modified in each of these ways retained catalytic activity and exhibited nuclease resistance in the presence of 10% fetal bovine serum. Enzymes with an inverted thymidylate at their 3′ terminus exhibited the best combination of catalytic activity and stability against nucleases (M. W. Anderson and G. F. Joyce, unpublished results).

The full scope of potential applications for the 10-23 DNA enzyme is presently unknown. These undoubtedly will include in vitro restriction digestion of RNA for the preparation of RNAs with a defined 3′ end or for probing RNA secondary and tertiary structure. If the challenges outlined above pertaining to the cellular application of the DNA enzyme can be overcome, this molecule may also prove to be a valuable instrument for the study of gene function and for gene inactivation at the level of RNA.

ACKNOWLEDGMENT

We thank Ronald Breaker, Martha Fedor, and Dan Herschlag for helpful comments on the manuscript. S.W.S. received support from the Corbin Foundation for Molecular Biology Research.

REFERENCES

1. Cech, T. R. (1992) *Curr. Opin. Struct. Biol. 2*, 605−609.
2. Long, D. M., and Uhlenbeck, O. C. (1993) *FASEB J. 7*, 25−30.
3. Symons, R. H. (1994) *Curr. Opin. Struct. Biol. 4*, 322−330.
4. Breaker, R. R., and Joyce, G. F. (1994) *Chem. Biol. 1*, 223−229.
5. Santoro, S. W., and Joyce, G. F. (1997) *Proc. Natl. Acad. Sci. U.S.A. 94*, 4262−4266.
6. Wincott, F., DiRenzo, A., Shaffer, C., Grimm, S., Tracz, D., Workman, C., Sweedler, D., Gonzalez, C., Scaringe, S., and Usman, N. (1995) *Nucleic Acids Res. 23*, 2677−2684.
7. Milligan, J. F., and Uhlenbeck, O. C. (1989) *Methods Enzymol. 180*, 51−62.
8. Herschlag, D., and Cech, T. R. (1990) *Biochemistry 29*, 10159−10171.
9. Fedor, M. J., and Uhlenbeck, O. C. (1992) *Biochemistry 31*, 12042−12054.
10. Hertel, K. J., Herschlag, D., and Uhlenbeck, O. C. (1994) *Biochemistry 33*, 3374−3385.
11. Knitt, D. S., and Herschlag, D. (1996) *Biochemistry 35*, 1560−1570.
12. Dahm, S. C., and Uhlenbeck, O. C. (1991) *Biochemistry 30*, 9464−9469.
13. Pan, T., Long, D. M., and Uhlenbeck, O. C. (1993) in *The RNA World* (Gesteland, R. F., and Atkins, J. F., Eds.) pp 271−302, Cold Spring Harbor Laboratory Press, Cold Spring Harbor, NY.
14. Fersht, A. (1985) *Enzyme Structure and Mechanism*, W. H. Freeman, New York.
15. Symons, R. H. (1992) *Annu. Rev. Biochem. 61*, 641−671.
16. Scott, W. G., and Klug, A. (1996) *Trends Biochem. Sci. 21*, 220−224.
17. Gerlt, J. A., Westheimer, F. H., and Sturtevant, J. M. (1975) *J. Biol. Chem. 250*, 5059−5067.
18. Hertel, K. J., and Uhlenbeck, O. C. (1995) *Biochemistry 34*, 1744−1749.
19. Hegg, L. A., and Fedor, M. J. (1995) *Biochemistry 34*, 15813−15828.
20. Prody, G. A., Bakos, J. T., Buzayan, J. M., Schneider, I. R., and Bruening, G. (1986) *Science 231*, 1577−1580.
21. Symons, R. H. (1989) *Trends Biochem. Sci. 14*, 445−450.
22. Buzayan, J. M., Gerlach, W. L., and Bruening, G. (1986) *Nature 323*, 349−353.
23. Burke, J. M. (1996) *Biochem. Soc. Trans. 24*, 608−615.
24. Stage-Zimmermann, T. K., and Uhlenbeck, O. C. (1998) *RNA 4*, 875−889.
25. Nelson, J. W., and Tinoco, I. (1982) *Biochemistry 21*, 5289−5295.
26. McConnell, T. S. (1997) *Biochemistry 36*, 8293−8303.
27. Pörschke, D., Uhlenbeck, O. C., and Martin, F. H. (1973) *Biopolymers 12*, 1313−1335.
28. Williams, A. P., Longfellow, C. E., Freier, S. M., Kierzek, R., and Turner, D. H. (1989) *Biochemistry 28*, 4283−4290.
29. Wetmur, J. G., and Davidson, N. (1968) *J. Mol. Biol. 31*, 349−370.
30. Manning, G. S. (1976) *Biopolymers 15*, 1333−1343.
31. Manning, G. S. (1978) *Q. Rev. Biophys. 11*, 179−246.
32. Pontius, B. W., and Berg, P. (1991) *Biochemistry 30*, 8237−8241.
33. Nedbal, W., and Sczakiel, G. (1996) *Biochem. Soc. Trans. 24*, 615−618.
34. Nedbal, W., Homann, M., and Sczakiel, G. (1997) *Biochemistry 36*, 13552−13557.
35. Albery, W. J., and Knowles, J. R. (1976) *Biochemistry 15*, 5631−5640.
36. Werner, M., and Uhlenbeck, O. C. (1995) *Nucleic Acids Res. 23*, 2092−2096.
37. Raillard, S.-A., and Joyce, G. F. (1996) *Biochemistry 35*, 11693−11701.
38. Xiang, Q., Qin, P. Z., Michels, W. J., Freeland, K., and Pyle, A. M. (1998) *Biochemistry 37*, 3839−3849.
39. Hertel, K. J., Peracchi, A., Uhlenbeck, O. C., and Herschlag, D. (1997) *Proc. Natl. Acad. Sci. U.S.A. 94*, 8497−8502.
40. Herschlag, D. (1991) *Proc. Natl. Acad. Sci. U.S.A. 88*, 6921−6925.
41. Hertel, K. J., Herschlag, D., and Uhlenbeck, O. C. (1996) *EMBO J. 15*, 3751−3757.
42. Sugimoto, N., Nakano, S., Katoh, M., Matsumura, A., Nakamuta, H., Ohmichi, T., Yoneyama, M., and Sasaki, M. (1995) *Biochemistry 34*, 11211−11216.
43. Zuker, M., and Stiegler, P. (1981) *Nucleic Acids Res. 9*, 133−148.
44. Jaeger, J. A. (1989) *Proc. Natl. Acad. Sci. U.S.A. 86*, 7706−7710.
45. Lieber, A., and Strauss, M. (1995) *Mol. Cell. Biol. 15*, 540−551.
46. Kawasaki, H., Ohkawa, J., Tanishige, N., Yoshinari, K., Murata, T., Yokoyama, K. K., and Taira, K. (1996) *Nucleic Acids Res. 24*, 3010−3016.
47. Birikh, K. R., Berlin, Y. A., Soreq, H., and Eckstein, F. (1997) *RNA 3*, 429−437.
48. Matveeva, O., Felden, B., Audlin, S., Gesteland, R. F., and Atkins, J. F. (1997) *Nucleic Acids Res. 25*, 5010−5016.
49. Milner, N., Mir, K. U., and Southern, E. M. (1997) *Nat. Biotechnol. 15*, 537−541.
50. Ho, S. P., Bao, Y., Lesher, T., Malhotra, R., Ma, L. Y., Fluharty, S. J., and Sakai, R. R. (1998) *Nat. Biotechnol. 16*, 59−63.
51. Patzel, V., and Sczakiel, G. (1998) *Nat. Biotechnol. 16*, 64−68.
52. Eckstein, F. (1998) *Nat. Biotechnol. 16*, 24.
53. Szymkowski, D. E. (1996) *Drug Discovery Today 1*, 415−428.

54. Stein, C. A., and Cheng, Y.-C. (1993) *Science 261*, 1004−1012.
55. Christoffersen, R. E., and Marr, J. J. (1995) *J. Med. Chem. 38*, 2023−2037.
56. Uhlmann, E., and Peyman, A. (1990) *Chem. Rev. 90*, 543−584.
57. Sharma, H. W., and Narayanan, R. (1995) *BioEssays 17*, 1055−1063.

BI9812221